UDK 621.791.724:621.98
Original scientific article/Izvirni znanstveni članek

ISSN 1580-2949
MTAEC9, 58(3)363(2024)

INVESTIGATION OF THE BENDING BEHAVIOR OF INC625/SUS316L LASER-CLADDING LAYERS APPLIED TO GGG40

OBNAŠANJE LASERSKO NANEŠENIH PLASTI INC625/SUS316L NA PODLAGO IZ NODULARNE LITINE VRSTE GGG40 POD UPOGIBNO OBREMENITVIJO

Ekrem Altuncu[1*], Melih Tarım[2]

[1]Sakarya University of Applied Sciences, Materials and Manufacturing Tech.App. and Research Center, Sakarya ,Türkiye
[2]Uniquetech Engineering, Kocaeli, Türkiye

Prejem rokopisa – received: 2023-12-12; sprejem za objavo – accepted for publication: 2024-04-12

doi:10.17222/mit.2023.1075

Laser cladding is a multi-purpose thermal coating technology whose application area has increased rapidly in recent years. It can be used for the purposes of obtaining a thick (mm to cm) layer on surfaces by the interaction of different materials in powder form (especially metallic and metal-matrix composite) with the laser beam, thus repairing, restoring, improving and protecting the surface resistance of various industrial metallic parts. It is normally used to refurbishment, create and repair metallic components, hydraulic mills, gears, shafts, turbine blades, drilling tools, and other static or dynamically loaded mechanical parts. The benefits of laser cladding over alternative technologies include better metallurgy (bonding, hardness or lower porosity) as well as reduced part deformation and stress due to lower overall heat input. The melting of substrate material ensures a good metallurgical bond between the cladding layer and the substrate material. However, the melting of the substrate material causes dilution. Therefore, the melting of the substrate material should be controlled and kept to a minimum because high substrate melting causes an increase in the dilution, which may degrade the mechanical and corrosion properties of the clad layer. The laser beam over the substrate materials creates temperature gradients in the thickness direction that can lead to mechanical deformation (such as bending) and changes in the microstructural and interface properties. Depending on the substrate type and production history, as well as the laser-clad powder properties and process parameters (power, feed rate, clad speed etc.) used in the application, the deformation properties of the cladded part and its bending behavior can change.
In this study, INC625 and SUS 316L+INC625 clad layers were applied on a GGG40 substrate with optimized parameters and then subjected to bending tests. Bending-test results were examined comparatively and their microstructural properties were examined. Cladding powder feedstock material properties, substrate type and its thermo-physical properties, clad process parameters and surface preparation conditions, number and thickness of layers are the most important factors affecting the bending behaviour in laser-cladding applications and require optimization studies. The INC625 clad layer on the SUS316L bond layer has reduced the diffusional effects, and the hardness distribution has a more homogeneous profile. In this way, an increase in bending angles was observed. The highest bending angle of 32° was measured with dublex-clad layered samples.

Keywords: Laser cladding, bending behaviour, dilution, microstructure, hardness

Laserska tehnologija nanašanja tankih plasti oziroma prekrivanje izbrane podlage je več namenski termični postopek prekrivanja, ki se v zadnjem času hitro razvija in že uporablja na številnih področjih. Lahko se uporabi za izdelavo relativno debelih plasti (mm do cm) na površinah različnih delov z interakcijo različnih materialov v obliki prahov (še posebej kovinskih ali kompozitov na osnovi matrice keramika-kovina). Z laserskim žarkom na ta način lahko popravimo, obnovimo, zaščitimo ali izboljšamo površino različnih industrijskih kovinskih delov. Običajno se postopek uporablja za obnovo, kreiranje ali popravilo kovinskih komponent, hidravličnih mlinov, valjev, zobnikov, gredi, turbinskih lopatic, vrtalnega orodja, in drugih statično ali dinamično obremenjenih mehanskih delov. Prednosti laserskega prekrivanja v primerjavi z drugimi alternativnimi tehnologijami so metalurške narave (boljša difuzijska vezava, trdota, manjša poroznost), kakor tudi manjše deformacije delov in manjše notranje napetosti zaradi manjšega celokupnega vnosa toplote. Raztaljeni material podlage zagotavlja dobro metalurško povezavo med z laserjem nanešeno plastjo in podlago. Vendar pa taljenje materiala podlage oziroma substrata povzroča povečano raztapljanje. Zaradi tega mora biti taljenje substrata kontrolirano oziroma čim manjše, ker le-to povzroča povečano raztapljanje, kar lahko povzroči poslabšanje mehanskih lastnosti in korozijskih lastnosti nanešene plasti. Laserski žarek povzroča nastanek temperaturnega gradienta v smeri debeline prekrivne plasti, kar lahko povzroči mehanske deformacije kot je krivljenje ali upogibanje, kakor tudi mikrostrukturne spremembe in spremembe lastnosti na meji med plastjo in substratom. V odvisnosti od vrste substrata in zgodovine izdelave, lastnosti prahu za lasersko prekrivanje in procesnih parametrov (moč, hitrost nanašanja itd.), ki so uporabljeni za določeno aplikacijo se deformacija lasersko obdelanih delov in njihovo upogibno obnašanje lahko spremeni.
V članku avtorji opisujejo lasersko nanešene plasti na osnovi INC625 in SUS 316L+INC625 na substrat iz nodularne litine vrste GGG40, ki so bile izdelane pri optimalnih procesnih parametrih. Sledilo so mehanski preizkusi preizkušancev pod upogibno obremenitvijo. Rezultate upogibnih preizkusov so medsebojno primerjali in izvedene so bile še mikrostrukturne preiskave. Lastnosti prahu za lasersko nanašanje, procesni parametri laserskega nanašanja in njegove termo-fizikalne lastnosti, pogoji priprave površine substrata, število in debelina plasti so najbolj pomembni faktorji, ki vplivajo na upogibne lastnosti lasersko izdelanih prevlek. Zato se zahteva izvedba natančne študije optimiziranja. Lasersko nanešena plast iz INC625 na SUS316L vezno plast je zmanjšala vplive difuzije in porazdelitev trdote po profilu nanosa je bila bolj enakomerna. Na ta način so dosegli povečanje upogibnega kota. Največji upogibni kot 32° so izmerili pri vzorcih z dupleks plastjo nanosa.

Ključne besede: lasersko prekrivanje, obnašanje pod upogibno obremenitvijo, raztapljanje, mikrostruktura, trdota

*Corresponding author's e-mail:
altuncu@subu.edu.tr (Ekrem Altuncu)

1 INTRODUCTION

Laser cladding has been a widely used surface-modification technology for metallic parts. The built-up layer using cladding technology has excellent restoration and protection performance, and the thickness of the cladding layers can be changed from 100 μm to a few centimeters. Laser-clad technology is also used in repairing worn surfaces, protecting surfaces against corrosion and oxidation, increasing wear life, increasing surface resistance and hardness, and producing 3D parts. The most important feature of this method can be shown that the clad layer has very good metallurgical bonding as in a welding build-up repair application, but has less dilution and a low heat-affected zone compared to the high heat input in welding or PTA processes.[1–7]

The laser beam, which acts on the substrate surface, creates a melt pool, and the fed powder material provides the formation of a clad layer in this region. There is a certain level of controllable heat input to the substrate surface. The heat-affected zone (HAZ) occurs in this region between the clad layer and the substrate. Structural features that can be controlled by process parameters include dilution, HAZ and interfacial microstructure features. The high heat input to the substrate changes the geometry and dimensions of the dilution zone. In this changing region, internal stresses affect the ductility and deformation ability of the material. Just like in welding processes, a high heat input should be avoided in laser-clad applications, internal stresses should be reduced in controlled layer development and interface properties. Serial hardness measurements have an important place in the microstructural control of internal stresses. The high hardness increase in the interface areas adversely affects the deformation of the material and the layer together and may cause cracking and fracture.[1–7]

The focus of Liu et al.'s experimental work is mainly on the structural properties of laser-coated In625/Steel structures and their interface evolution over heat and/or chemical treatments. In general, in the first layer application, the process parameter design on the steel surface should be made appropriately. It is recommended to increase the powder feed rate and/or decrease the laser power to reduce undesired dilution ratios. Observations provide evidence that both the carbide precipitations and the local strains play an important role in the interface stability of the laser-cladded In625/Steel structures upon heat and/or chemical corrosion.[8]

The studies of Xu et al. are on single-bead and multiple-bead Inconel 625 coatings were fabricated on the surface of 316L stainless steel by laser cladding. The cladded area and the bonding area exhibited superior tensile properties at both room temperature and high temperature than the substrate. The corrosion performance of the coating area was also close to the bonding area and superior to the substrate in different solutions.[9] Ni-based superalloy Inconel 625 (IN625) has been one of the most widely used nickel-based alloys in aviation, chemical and marine applications due to its excellent corrosion and high-temperature corrosion resistance, as well as its high yield strength, creep strength and fatigue strength. For the surface modification industry, Inconel 625 is also utilized extensively as a coating material for corrosion environments and for the hard-facing of tool and die steels.[9]

Abioye et al.'s study is on the electrochemical corrosion performance of laser-clad Inconel 625 wire in a de-aerated 3.5 *w*/% NaCl solution. Well bonded, minimally diluted, pore- and crack-free single beads and multiple (overlapped) beads of Inconel 625 wire were successfully deposited. The microstructural evolution of a typical clad bead is observed to begin with columnar dendrites, at the clad-substrate interface, growing vertically to the substrate. The corrosion performance of the coating, which degrades with increasing Fe dilution, is very close to that of wrought Inconel 625, but superior to wrought 304L stainless steel.[10]

Nakki and et al.'s study results showed that powders containing the lowest amount of impurity elements (S, P, B) were the most resistant to hot cracking. Ti and Al were beneficial if the impurity element contents were high.[11]

Olakanmi and et al.'s process-optimization studies are on fiber-laser cladded Inconel-625 composite coatings. The dilution ratio was minimised as the coating's microhardness and the process efficiency were maximised with an appropriate combination of laser energy density, inconel content and shielding gas flow rates.[12]

Abioye et al. studied the parametric process parameters of Inconel 625 wire laser deposition. Laser power energy density per unit length of track was found to be the key parameter influencing both the process and the track geometrical characteristics.[13]

As can be seen, both the process parameters and the substrate type, as well as the laser clad dilution ratios and interface charactristics, control the physical and chemical properties of the clad layer.

N-GJS-400-15C, also known as GGG40, is one of the most used nodular cast iron grades and has a predominantly ferritic structure. This grade offers superior machinability combined with good impact resistance, good elongation properties. This material is suitable for various applications within the industries of automotive, machinery, hydraulics and pneumatics, pumps and compressors, oil and gas along with equipment for steel manufacturing. Ductile cast iron is hard to remanufacture without preheating and post heat treatment owing to the complicated phase evolution and a great tendency to form chilled structure during the cladding process.[14]

The surface of the ductile cast iron was often damaged due to strong wear and impact during service resulting in failure of the ductile cast iron. A variety of ways were used to remanufacture those damaged workpieces such as shielded metal arc, TIG and other repair welding methods. However, due to the poor weld-

Table 1: Material Compositions

GGG40 EN-GJS-400-15	Substrate		
	C 3.4-3.85, Si 2.3-3.1, Mn 0.1-0.3 S 0.02max, P0.10 max, rest Fe		
INC 625	Cladding powders	Powder size	Form
	Ni <0.03C 0.4Si 0.75Fe 21.5Cr 9Mo 3.7Nb	125/45 μm	Gas atomized Globular form
SUS 316L	Fe <0.03C 1.6Si 17Cr 12Ni 2.5Mo 1.5Mn	150/53 μm	

ability of ductile cast iron, lots of problems could not be solved using these methods, such as wide fusion region with high hardness, strong tendency of cracking and chilled structure, high heat input and large tendency of deformation. During the remanufacturing process, it is a key problem to control the diffusion of carbon close to the interface region and control the precipitation of the brittle phases in the partially melted zone and the heat-affected zone.[15]

Therefore, within the scope of this study, the bending behavior of single-layer (INC 625) and double-layer (SUS316L / INC625) laser clad layers on ductile cast iron (GGG40), depending on the interface properties, was investigated.

2 EXPERIMENTAL PART

In the experimental studies, a single layer INC625 layer and a double layer SUS316L+INC625 layer were formed on the GGG40 nodular cast iron substrate. The laser clad process was carried out robotically with a 4.4-kW fiber diode laser (Erlas, Laserline) system in **Figure 1a**. **Figure 1b** shows the cladding process schematically. The cladding zone, the heat-affected zone and the dilution zone are indicated. Test specimens produced with different layer thicknesses were subjected to bending loads and their deformation behavior and fracture surfaces were investigated.

EDX analysis studies were carried out with electron microscopy (SEM, Tescan) in the microstructural characterization of the coating layers. Compositional changes at the interface were investigated with the element-mapping technique. A micro Vickers ($HV_{0.3}$, Schimadzu) hardness test was applied for the mechanical properties of the coatings, substrate and their interfaces. **Table 1** shows the chemical compositions of the substrate and powder materials used in the experimental studies.

Table 2 shows the system and optimized process parameters used in the production of laser-clad layers. A 6-axis KUKA robot system was used to control the movement of the laser head and the nozzle.

Table 2: Optimized process parameters and cladding unit

Powder Type	Power W	Cladding Speed mm/s	Powder feed rate g/min/min^{-1}
INC 625	1400	13	250 /2.5
SUS 316L	1350	15	200/2

Inert Ar gas was chosen as a powder carrier gas and the shielding gas, and N_2 gas was selected to protect the lens. The cladding region was machined and polished with sand paper (1200 MESH) and then cleaned with alcohol.

Figure 2 shows the bending-test samples (100 × 20 × 10) mm^3 produced by the laser-cladding process. Three-point bending tests were carried out according to the BS-ISO-EN 7438-2020 standard and then bending angle measurements were carried out (**Figure 3**). Each test was performed on three samples and the average value was taken. In the bending test, the bending angle of

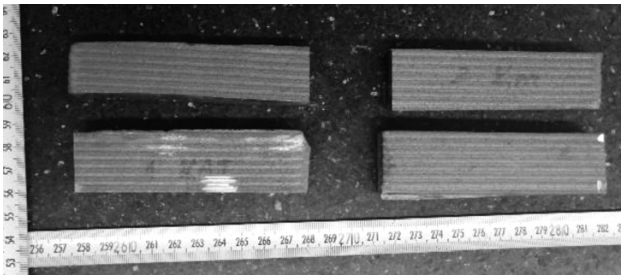

Figure 2: Images of laser-cladded bending-test samples

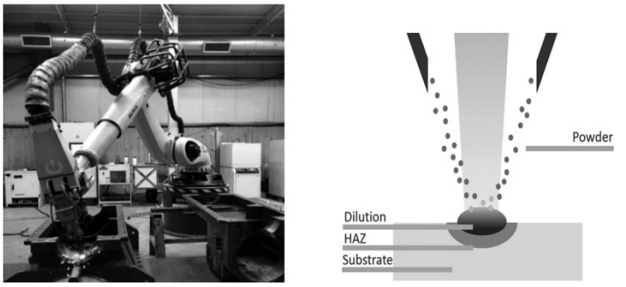

Figure 1: Laser cladding unit and process: a) Erlas laser-cladding unit, b) laser cladding process (schematic)

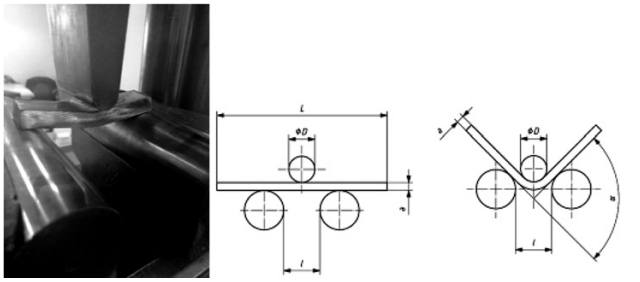

Figure 3: Bending test[14]

the clad specimen with different layers of different thickness was measured.

3 RESULTS AND DISCUSSION

3.1 Microstructures of clad layers

Figure 4 shows the typical microstructure of an INC625 clad layer on a GGG40 substrate. The clad layer thicknesses are 750–1050 ± 15 μm and there are some micro porosities (black dots indicated by arrow). The pore can be induced by the trapped gas in the cladding during the cooling of the molten powders. In the SEM-EDX analysis on the microstructure, element distributions taken from different points can be seen in **Figure 4a**. At the interface of the clad layer and the substrate, a diffusion zone and a heat-affected zone can be seen just below it. The formation of an intermetallic characteristic region is observed with Ni-Fe mutual atomic movements. Ni and Fe are thought to form intermetallic structures, especially in the transition zone from the nickel-based clade layer to the substrate. The results from points 5 and 6 in the EDX analysis prove this in **Figure 4b**.

Figure 5 shows the analysis performed by EDX-mapping method along the clad cross-section. The distribution of three main elements (Fe, Ni, Cr) can be clearly seen in the element mapping. Element transition points are observed in the transition interface regions. The cast-iron base is rich in Fe, the transition zone is a diffusional zone with Fe, Ni and Cr and the clad zone is rich in Ni and Cr.

Figure 6 shows a double-layered clad layer. Just above the substrate is SUS316L austenitic stainless steel

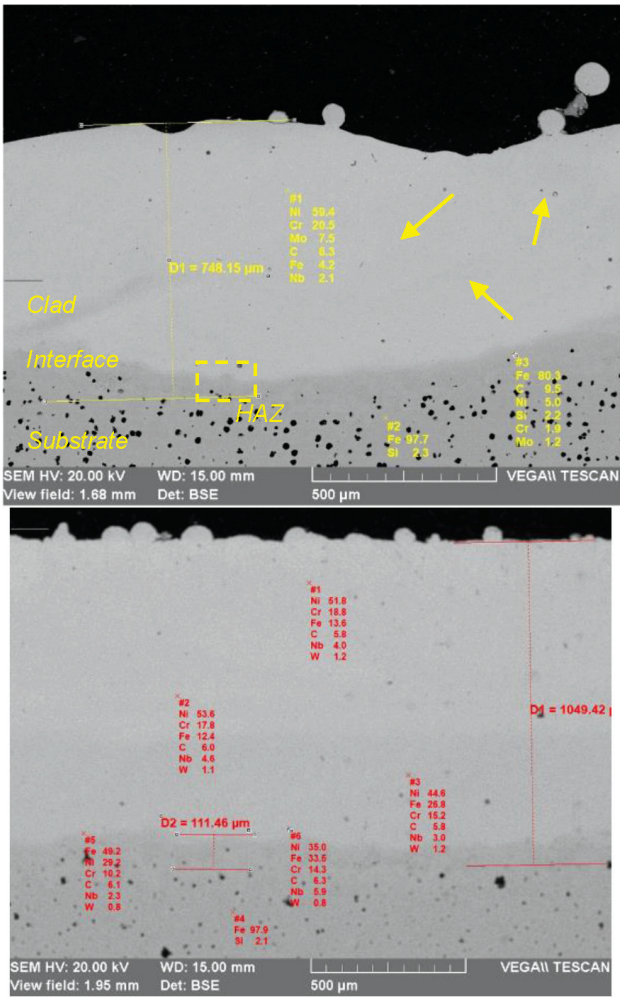

Figure 4: Microstructures of INC625 clad layers with EDX analysis: a) lower thickness, b) greater thickness

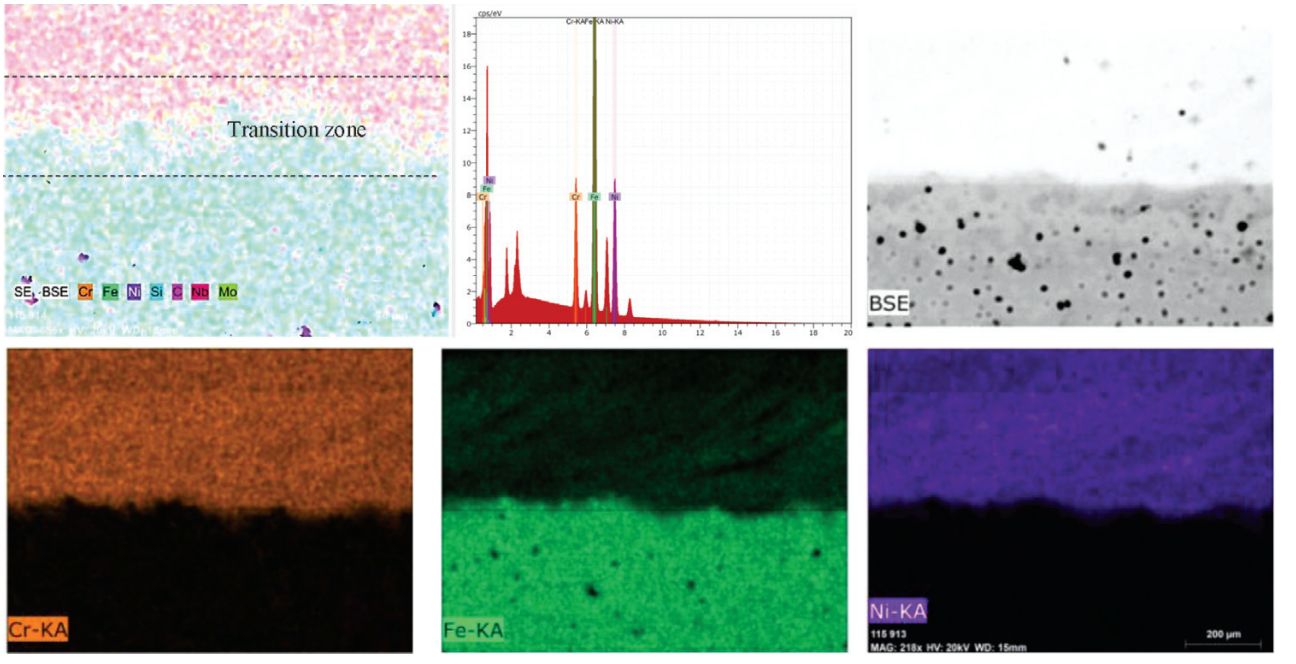

Figure 5: EDX mapping for Ni, Cr and Fe for INC625 clad on GGG40

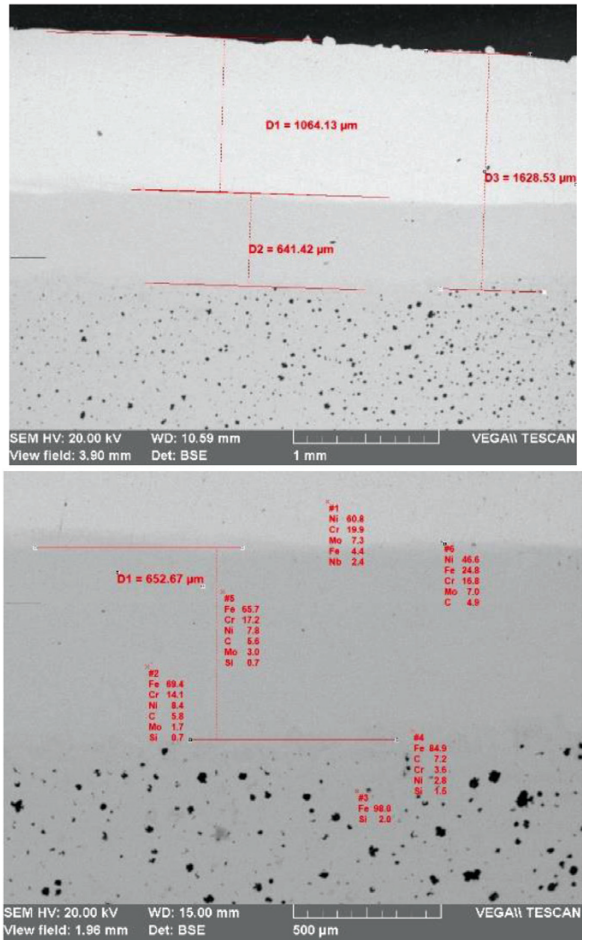

Figure 6: Microstructures of 316L+INC625 clad layers with EDX analysis: a) total thickness, b) interfaces and EDX analysis

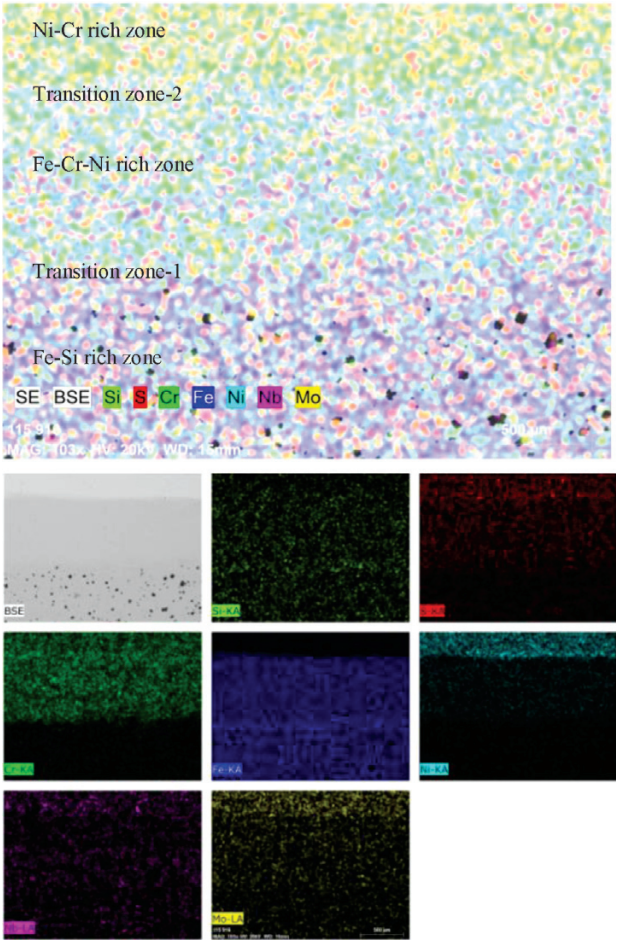

Figure 7: EDX mapping for Ni, Cr, Fe and other elements for SUS316l+INC625 clad on GGG40

and above it is a layer of INC 625 nickel-based superalloy clad layer. The total duplex clad-layer thickness is 1630 ± 15 µm (**Figure 6a**). The stainless-steel layer acts as a bond layer (625 ± 10 µm) for the Inconel clad layer with a thickness of 1035 ± 15 µm. In the EDX analysis, the diffusion of Ni and Fe is observed at the interface (**Figure 6b**) of the top layer and the bond layer. On the other hand, it was determined that diffusional changes were less at the SUS316 bond layer and the substrate interface (**Figure 7**).

3.2 Microhardness Profile of Clad Layers

No macro-sized discontinuities were observed in the microscopic examination of the cladding layers. Vickers microhardness ($HV_{0.3}$) measurements were made in a series of vertical and horizontal directions in the clad layer. Starting from the top layer, interfacial and substrate hardness measurements were carried out. Microhardness changes were observed, especially in the diffusion transition zones. During the formation of the clad layer with a laser beam, the element diffusion shows a hardening effect in the interfacial regions with the effect of the heat load on the substrate. The Ni towards the substrate and the Fe towards the clad layer mutually diffused and it is predicted that this caused the formation of intermetallic structures in the intermediate region. The effects of these phases are dominant in the sudden increase in hardness at the interfaces.

Also, the residual stresses can occur by the thermal expansion mismatch between the substrate and the clad-

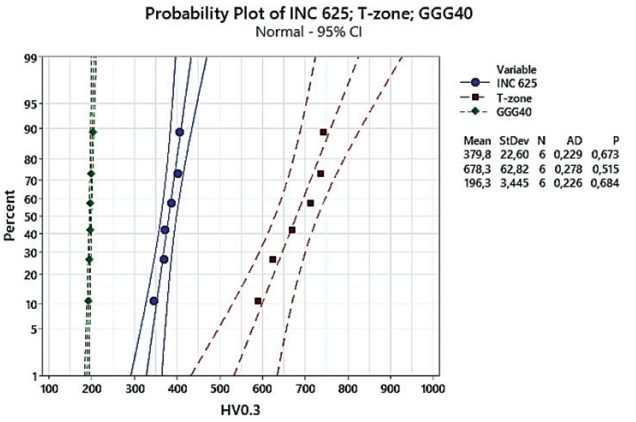

Figure 8: Probability of microhardness profile for INC625 clad on GGG40

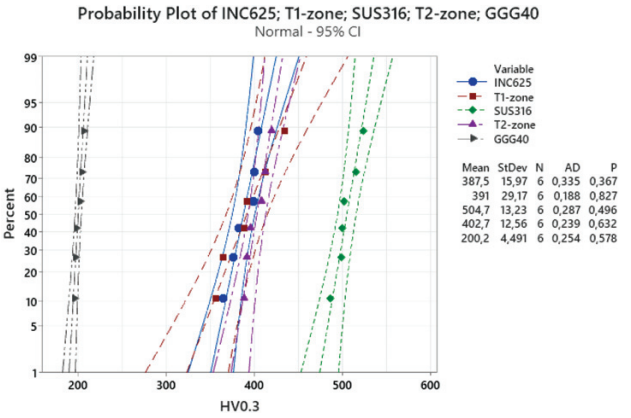

Figure 9: Probability of microhardness profile for SUS316L+INC625 clad on GGG40

Table 3: Bending-Test Results

Run Groups	Bending Angle	OK/ NOK
1-INC625 low thickness	<20°	NOK
2-INC625 high thickness	<12°	NOK
3-SUS316L+INC625 dublex clad layer	>25°	OK Acceptable
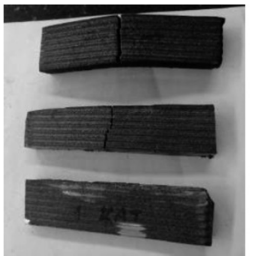		

ding materials during the cooling process of the claddings. Compared with the substrate, the expansion process of the cladding layer is more obvious. Therefore, fracture always occurred in the interface zone and cladding layers if the residual stress was high enough.[15]

As can be seen in **Figure 8**, the average microhardness values are 196 ± 4$HV_{0.3}$ for GGG40 as substrate, 678 ± 62$HV_{0.3}$ for T-zone (interface), and 379 ± 20 $HV_{0.3}$ for INC625 clad layer, respectively. A significant increase in hardness is observed in the interfacial region. Microstructural phase transformations affect the hardening of this region. Such a hardness difference between the clad layer and substrate interface naturally changes the thermal expansion behaviours and the deformation capability.

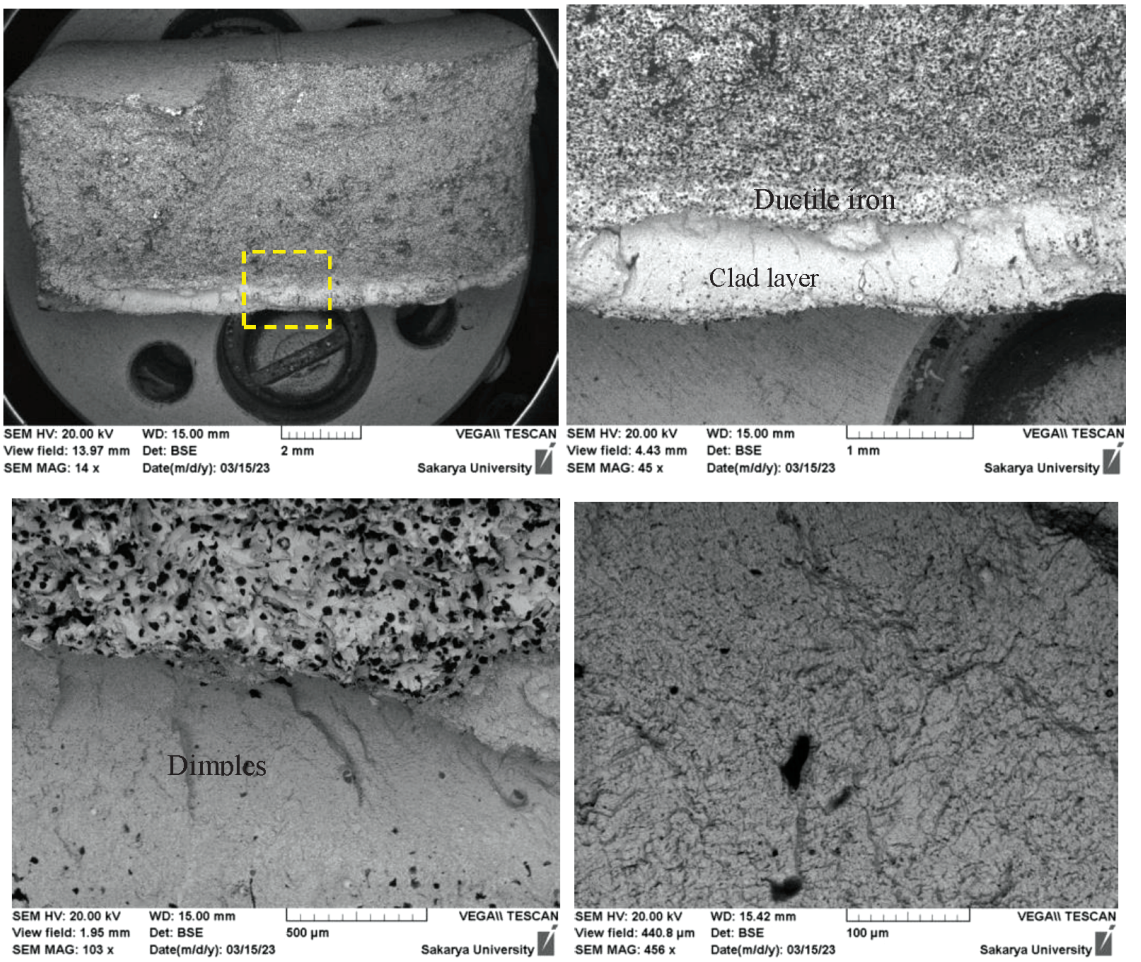

Figure 10: Fracture-surface images after bending test

As can be seen in **Figure 9**, the average microhardness values are 200 ± 5 $HV_{0.3}$ for GGG40 as substrate, 402 ± 12 $HV_{0.3}$ for T2-zone (SUS316-Substrate interface), and 504 ± 13 HV0.3 for SUS316L clad layer, 391 ± 29 $HV_{0.3}$ for T1-zone (SUS316-INC625 interface), 387 ± 16 $HV_{0.3}$ for INC625 clad layer. As can be seen from the average hardness values and distribution, the increase in the interfacial hardness with the application of SUS316 bond layer shows relatively lower hardnesses compared to the application of Inconel 625.

3.3 Results of the Bending Tests

Three different groups of bending-test specimens were tested, and the tests were repeated three times. The test was terminated when the first crack started after the load was applied. Bending angles were measured with a digital angle gauges (**Table 3**). The effect of the layer thickness on the bending deformation ability is clearly seen. It was observed that the thick INC625 clad layer was more rigid than the thinner INC625 layer and could not respond to bending loads. Hardening in the interface zone and additional residual stresses are thought to limit the deformation. On the other hand, it was observed that the two-layer duplex-clad layer showed a better deformation.

3.4 Fractographic Examinations

The surfaces of the parts that were broken as a result of the bending test were examined under the electron microscope (SEM). The fracture-surface images are displayed at different magnifications in **Figure 10**. The appearance of the fracture surface is quasi cleavage, composed by zones with ductile fractures and facets of cleavage (**Figures 10a**, **10b**). Crack initiation and propagation occur immediately, with the fracture propagating through the entire test specimen. The dimple shape (**Figure 10c**) is governed by the state of stress within the cross-section as the microvoids grow and coalesce in the ductile iron. The result is a typical cleavage surface for a clad layer (**Figure 10d**).

4 CONCLUSIONS

To summarize, the type of powder material used in the laser-clad process, the type of substrate, layer thicknesses and layer design are among the effective factors in the bending behaviour of laser-clad test plates. The bending angles are below 20 degrees for single-layer INC625 layers. The average hardness value is about 380 $HV_{0.3}$ in the INC625 cladding layers. The interface zone near the external surface of the cladding layers showed the highest hardness value, which is close to 750 $HV_{0.3}$. The hardness in the interface zone is strongly dependent on the phases. The hardness will increase with the increasing of martensite percentage in the interface zone. It cannot respond to bending loads due to the increase in the interfacial stiffness. Although the reduction of the layer thickness partially reduces the thermal expansion mismatch, diffusional interactions during the laser-clad process increase the hardness by causing the formation of interfacial intermetallic (Ni-Fe) compounds. On the other hand, the INC625 clad layer on the SUS316L bond layer reduced the diffusional effects, and the hardness distribution has a more homogeneous profile. In this way, an increase in bending angles was observed. The highest bending angle of 32° was measured. In ductile iron without clad layer, the bending angle is 35°.

Acknowlodgement

The authors would like to thank the Management of Uniquetech Engineering for their support and contribution to this study.

5 REFERENCES

[1] T. Han, K. Zhou, Z. Chen, Y. Gao, Research Progress on Laser Cladding Alloying and Composite Processing of Steel Materials. Metals 12 (**2022**), 2055, 1–18, doi:10.3390/met12122055

[2] J. Zeng, G. Lian, M. Feng, Z. Lin, Inclined shaping quality and optimization of laser cladding. Optik 266 (**2022**), 169598, 1–14, doi:10.1016/j.ijleo.2022.169598

[3] G. Piscopo, L. Iuliano, Current research and industrial application of laser powder directed energy deposition. Int J Adv Manuf Technol 119 (**2022**), 6893–6917, doi:10.1007/s00170-021-08596-w

[4] H. Zhang, Y. Pan, Y. Zhang, G. Lian, Q. Cao, J. Yang, Influence of laser power on the microstructure and properties of in-situ NbC/WCoB–TiC coating by laser cladding. Mater. Chem. Phys. 290 (**2022**), 126636, doi:10.1016/j.matchemphys.2022.126636

[5] W. Kai-Ming, F. Han-Guang, L. Yu-Long, L. Yong-Ping, W. Shi-Zhong, S. Zhen-Qing, Effect of power on microstructure and properties of laser cladding NiCrBSi composite coating. Trans. IMF, 95 (**2017**), 328–336, doi:10.1080/00202967.2017.1355640

[6] D. M.Goodarzi, J. Pekkarinen, A. Salminen, Analysis of laser cladding process parameter influence on the clad bead geometry, Weld. World 61 (**2017**), 883–891, doi:10.1007/s40194-017-0495-0

[7] M. Nie, S. Zhang, Z. Wang, C. Zhang, H. Chen, J. Chen, Effect of laser power on microstructure and interfacial bonding strength of laser cladding 17-4PH stainless steel coatings. Mater. Chem. Phys. 275 (**2021**), 125236, DOI:10.1007/s11665-022-07484-y

[8] H. Liu, Chee K. Ivan Tan, Y.Wei, S. H. Lim, J. Coryl, J. Lee, Laser-cladding and interface evolutions of inconel 625 alloy on low alloy steel substrate upon heat and chemical treatments, Surf. Coat. Tech. 404 (**2020**) 25, 126607, doi:10.1016/j.surfcoat.2020.126607

[9] X. Xu, G. Mi, L. Chen, L. Xiong, P. Jiang, X. Shao, C. Wang, Research on microstructures and properties of Inconel 625 coatings obtained by laser cladding with wire, J. Alloys Compd., 715 (**2017**), 362–373, DOI10.1016/j.jallcom.2017.04.252

[10] T. E. Abioye, D. G. McCartney, A. T. Clare, Laser cladding of Inconel 625 wire for corrosion protection, J. Mater. Process. Technol., 217 (**2015**), 232–240, doi:10.1016/j.jmatprotec.2014.10.024

[11] J. Näkki, J. Tuominen, P. Vuoristo, Effect of minor elements on solidification cracking and dilution of alloy 625 powders in laser cladding J. Laser Applic., 29 (**2017**), Article 012014, doi:10.2351/1.4973673.

[12] E. O. Olakanmi, S. T. Nyadongo, K. Malikongwa, S. A. Lawal, A. Botes, S. L. Pityana, Multi-variable optimisation of the quality characteristics of fiber-laser cladded Inconel-625 composite coatings,

Surface and Coatings Technology, 357 (**2019**), 289–303, doi:10.1016/j.surfcoat.2018.09.063

[13] T. E. Abioye, J. Folkes, A. T. Clare, A parametric study of Inconel 625 wire laser deposition, Journal of Materials Processing Technology, 213 (**2013**) 12, 2145–2151, doi:10.1016/j.jmatprotec.2013.06.007

[14] BS-ISO-EN 7438-2020 Metallic materials. Bend test. BSI Standards Publication, UK

[15] Y. Li, S. Dong, S. Yan, X. Liu, P. He, B. Xu, Surface remanufacturing of ductile cast iron by laser cladding Ni-Cu alloy coatings, Surface and Coatings Technology, 347 (**2018**), 20–28, doi:10.1016/j.surfcoat.2018.04.065